Lasers in Surgery and Medicine 38:555–564 (2006)

Multicell Tumor Spheroids in Photodynamic Therapy

Steen J. Madsen, PhD,[1,2]* Chung-Ho Sun, PhD,[3] Bruce J. Tromberg, PhD,[3] Vittorio Cristini, PhD,[4] Nzola De Magalhães, MS,[3] and Henry Hirschberg, MD, PhD[1,3,5]

[1]*Department of Health Physics, University of Nevada, Las Vegas, Nevada*
[2]*University of Nevada, Las Vegas Cancer Research Center, Las Vegas, Nevada*
[3]*Beckman Laser Institute, University of California, Irvine, California 92612*
[4]*Department of Biomedical Engineering, University of California, Irvine, California 92697*
[5]*Department of Neurosurgery, Rikshospitalet/Radiumhospital, Oslo, Norway*

Background and Objectives: Multicell spheroids (MCSs) represent a simple in vitro system ideally suited for studying the effects of a wide variety of investigational treatments including photodynamic therapy (PDT).

Study Design/Materials and Methods: In the first section of this review study, an overview of the current literature on MCS in PDT will be presented. Knowledge of basic PDT parameters has been gained from numerous MCS studies, in particular, the mechanisms of sensitizer photobleaching have been elucidated. MCSs have also proven useful for the study of complex PDT treatment regimens including multiple treatments and combined therapies involving PDT and ionizing radiation or hyperthermia. The purpose of the second part of this review is to present results from recent studies in our laboratory aimed at developing MCS models suitable for investigating tumor cell invasion and angiogenesis—processes characteristic of high-grade gliomas.

Results and Conclusion: To that end, progress has recently been made to develop a more accurate in vivo brain tumor model consisting of biopsy-derived human tumor spheroids implanted into the brains of immunodeficient rats. Finally, recent work suggests that computer simulations may prove useful to describe the growth of MCS and predict the effects of investigational therapies including PDT. Such in silico models have made a number of counterintuitive predictions that have been verified in vitro and, as such, could guide the development of improved therapeutics. Lasers Surg. Med. 38:555–564, 2006. © 2006 Wiley-Liss, Inc.

Key words: multicell spheroids; photodynamic therapy; brain tumor; glioblastoma multiforme; chick chorioallantoic membrane; in silico spheroid model

INTRODUCTION

Multicell spheroids (MCSs) are three-dimensional aggregates of cells that mimic micro-tumors and metastases. Sutherland et al. [1,2] were the first to use this in vitro model for the systematic study of tumor response to therapy. These early pioneering studies provided the impetus for using MCS to study the effects of a wide variety of therapies on fundamental biological mechanisms, including regulation of proliferation, cell death, differentiation, metabolism, invasion, immune response, and angiogenesis [3]. In comparison to monolayer cultures, a significant advantage of MCS is that their micro-environment more closely mimics the in vivo situation and therefore, gene expression and the biological behavior of the cells are likely similar to that encountered in tumor cells in situ.

Measurement of oxygenation gradients in MCS has been the subject of a number of studies [4–8]. Not surprisingly, MCSs show a radial decrease in oxygen partial pressure from the spheroid periphery towards the center. Depending on spheroid size and cell type, hypoxic cells are typically found either in the spheroid core, or in the rim surrounding the necrotic core with oxygen tensions typically below 10-mm Hg [5,8,9]. The conditions required for the development of the necrotic core are not well-understood, but are likely due to a number of factors including hypoxia [10]. The distance from the periphery of the spheroid at which necrosis occurs may vary from 50 to 300 μm, depending on cell type, substrate consumption rates, substrate concentrations in the growth medium, and cell packing densities [3]. For most types of human cells grown under optimal nutrient and oxygen conditions, the thickness of the viable rim of cells surrounding the necrotic core ranges from 100 to 220 μm [3]. In general, most of the proliferating cells in spheroids are found in the outer three to five cell layers (ca. 75 μm). The quiescent cells are located more centrally and can be recruited back into the cycling population under the appropriate environmental conditions.

The oxygen gradients characteristic of MCS produce a heterogeneous population of cells that differ in their response to oxygen-dependent therapies, such as ionizing radiation and photodynamic therapy (PDT). In addition to oxygenation status, tumor response to these therapies is controlled by a number of parameters including intracellular contact and communication and susceptibility to apoptosis [11]. Clearly, monolayer cultures are inadequate for investigating these parameters since they are unable to mimic oxygen gradients and the complex intracellular adhesion found in three-dimensional spheroids. In addition,

*Correspondence to: Steen J. Madsen, PhD, Department of Health Physics, University of Nevada, Las Vegas, 4505 Maryland Pkwy., Box 453037, Las Vegas, NV 89154-3037.
E-mail: steen.madsen@unlv.edu
Accepted 21 March 2006
Published online 19 June 2006 in Wiley InterScience (www.interscience.wiley.com).
DOI 10.1002/lsm.20350

the lack of an extracellular matrix in monolayer cell suspensions affects their response to a wide variety of therapies. In view of the findings that survival and cell death, especially apoptosis, depend strongly on both cell adhesion and the presence of an extracellular matrix [12], results obtained in monolayers are likely not a true indicator of therapeutic efficacy in vivo.

MCS IN BASIC PDT STUDIES

PDT efficacy depends on a number of parameters including tissue oxygenation status, photosensitizer concentration, light dose and dose rate, and the intrinsic sensitivity of the target tissue to the PDT effect. Accurate in vivo PDT dosimetry is complicated by the inherent difficulties associated with measuring these parameters. A number of alternative non-invasive dosimetry strategies, including measurements of sensitizer photobleaching, have been proposed [13]. MCSs represent an ideal system for investigating basic dosimetric PDT parameters, such as photobleaching and hence, data obtained in this model can be used to optimize treatments. A significant simplifying feature of MCS is that such basic studies can be accomplished in the absence of complex host-dependent factors, such as the tumor vasculature.

The first reported use of MCS as an in vitro model system for PDT was by Christensen et al. [14] in 1984. This, and other early studies, focused mainly on evaluating hematoporphyrin (Hpd) distributions and the effects of Hpd–PDT in a variety of MCS models [15–19]. In particular, fundamental studies by West [16] and West et al. [19] demonstrated that human colon carcinoma spheroids were more resistant to Hpd–PDT compared to monolayers and that the sensitivity to PDT decreased with increasing spheroid size. Furthermore, it was shown that PDT sensitivity was dependent on intracellular drug uptake within the spheroid. This finding has been confirmed in recent studies on mTHPC-loaded Colo 26 spheroids [20] and RT112 transitional cell carcinoma spheroids incubated in hypericin [21]. In both studies, high drug concentrations were observed at the spheroid periphery with a 5- to 10-fold decline 50 μm from the periphery. This is a more rapid decline than that observed for Photofrin which, in comparison, has relatively good overall penetration in spheroids [16].

Recently, MCSs have been used to investigate the diffusion kinetics of a number of second-generation photosensitizers and pro-drugs [21,22]. In particular, efforts have been aimed at improving the penetration of hydrophilic molecules such as 5-aminolevulinic acid (ALA) in biological tissues. This may be accomplished in a relatively straightforward manner by the addition of lipophilic ester groups, including butyl and hexyl chains [23]. Fluorescence microscopy has been used to evaluate ALA- and hexyl-ALA-induced protoporphyrin IX (PpIX) distributions in EMT6 spheroids [22]. It was observed that comparable levels of PpIX fluorescence could be achieved throughout the spheroids with 100-fold lower hexyl-ALA concentrations compared to ALA. The results also demonstrated that PpIX distributions resulting from hexyl-ALA were more uniform than those observed with ALA. Taken together, these results are consistent with the findings of Hirschberg et al. [24] who demonstrated that an equivalent response of human glioma spheroids to PDT with lipophilic ester derivatives (butyl-ALA and hexyl-ALA) could be achieved at concentrations 10- to 20-fold lower than that observed with ALA.

The PDT effect is sensitively dependent on the presence of oxygen during treatment. Unfortunately, the treatment itself may induce hypoxia due to consumption of singlet molecular oxygen ($^1O_2$)—the primary cytotoxic species. As shown by Foster et al. [25], in EMT6 murine mammary carcinoma spheroids, the effects of Photofrin-PDT are strongly dependent on the incident light fluence rate: lower fluence rates result in decreased spheroid survival. The increased efficacy of low fluence rate PDT has also been confirmed in human glioma spheroids using ALA [26] and Foscan-loaded human adenocarcinoma HT29 spheroids [27].

The concept of PDT-induced photochemical oxygen consumption has been investigated extensively by Georgakoudi et al. [28–30]. In particular, these investigations have used MCS to study sensitizer photobleaching during PDT which has resulted in a better understanding of singlet and non-singlet oxygen-mediated mechanisms of photobleaching. A thorough understanding of these mechanisms is a requirement for accurate non-invasive PDT dosimetry schemes based on photobleaching [13]. These studies have clarified the relationship between fluence rate and the PDT effect. For example, in the self-sensitized singlet oxygen-mediated bleaching model [28] the details of the spatial distribution of $^1O_2$ and, therefore of bleaching, depend on the fluence rate. The central prediction of this model is that, at a particular depth, $^1O_2$ concentration increases as fluence rates decrease and therefore, photodynamic damage will extend further into the spheroid as the fluence rate is lowered. Therefore, PDT with sensitizers, such as Photofrin and ALA-induced Pp IX which bleach via $^1O_2$, will result in improved therapeutic response at low fluence rates since $^1O_2$ is delivered to a larger volume of tumor cells.

The results of recent in vivo studies suggest that the kinetics of Photofrin photobleaching are more complex than that predicted by the $^1O_2$-mediated bleaching model. Consequently, a detailed investigation was initiated in EMT6 spheroids to better understand the mechanisms of Photofrin photobleaching [31]. The results suggest that the sensitizer bleaches via two simultaneous bleaching mechanisms consisting of: (1) reactions between $^1O_2$ and the drug, and (2) reactions between the sensitizer triplet and biological targets. For a given oxygen concentration, the relative importance of the two bleaching mechanisms depends on the initial concentration of the sensitizer. For example, at high drug concentrations, photobleaching proceeds primarily through reactions involving $^1O_2$. As the initial sensitizer concentration is decreased, there is a shift to sensitizer triplet reactions. There are significant dosimetric consequences of multiple simultaneous bleaching mechanisms. In particular, the model predicts that

real-time dosimetry based on spectroscopic monitoring of fluorescence photobleaching is only accurate at high sensitizer concentrations where bleaching is always $^1O_2$-mediated. In contrast, under conditions of low drug concentrations, triplet-mediated bleaching becomes important and the accumulation of photoproducts may be a more useful dosimetry metric than photobleaching.

MCS IN REPETITIVE PDT STUDIES

Clinical PDT investigations have traditionally involved single treatments. MCSs represent a simple system ideally suited for fundamental studies of more complex PDT treatments including fractionated and repetitive schemes. In order to avoid unacceptable sensitizer build-up, such treatments require drugs with rapid systemic clearance such as ALA. The effects of repetitive ALA-mediated PDT have been investigated in a human glioma spheroid model [32]. Significant inhibition of spheroid growth was observed during multiple weekly or bimonthly PDT treatments using sub-threshold light fluences. The increased efficacy of multiple PDT treatments was attributed to repeated destruction of the most sensitive cells in the outer layer of the spheroid, that is, the well-oxygenated proliferating cells. Cells of the outer layer have also been shown to produce the highest levels of photosensitizer [22]. As a result, the outer layer of cells is preferentially destroyed and slough off between treatments thereby inhibiting spheroid growth. As the outer layer is destroyed, viable non-proliferating cells are recruited into the proliferating pool and spheroid growth commences. Of particular interest is the observation that the surviving cells can be used to form a new generation of spheroids which are highly sensitive to renewed PDT. This phenomenon probably occurs in surgically treated tumors, such as glioblastoma multiforme (GBM) and demonstrates the importance of repeated access to the tumor bed over extended periods to allow for multiple treatments. Such extended treatments may necessitate the development of specially designed indwelling applicators to facilitate repeated access to the tumor bed [33].

COMBINATION THERAPIES

Investigations of the effects of combination therapies are complicated by the large number of parameters that must be considered. Consequently, most such studies have been performed in monolayer cell cultures under well-oxygenated conditions. The clinical relevance of such studies is highly questionable, especially when investigating the effects of oxygen-dependent therapies, such as PDT and ionizing radiation. Since MCSs are characterized by steep oxygen gradients, not unlike those found in tumors, they would appear to be ideally suited for the investigation of a wide range of combination therapies.

PDT and Ionizing Radiation

Knowledge of potentiation effects between PDT and ionizing radiation is clinically relevant since many patients undergoing investigative PDT are also likely to receive ionizing radiation. In a study investigating the effects of ionizing radiation and ALA-PDT on human glioma spheroids, the degree of interaction between the two modalities was shown to be sensitively dependent on a number of parameters including light fluence, fluence rate, and dose of gamma radiation [34]. It was shown that gamma radiation and PDT interact synergistically only if both light fluence and radiation dose exceed approximately 25 J/cm^2 and 8 Gy, respectively. Synergism was observed only at the lowest fluence rate (25 mW/cm^2) investigated. The degree of interaction was found to be independent of both treatment sequence and light intervals investigated (1 and 24 hours). TUNEL assays demonstrated that low fluence rate PDT was a very efficient inducer of apoptosis, whereas neither high-fluence rate PDT nor gamma radiation induced significant apoptosis. The preferential induction of apoptosis at low fluence rates has also been observed in Foscan-loaded HT29 spheroids [27]. Although the mechanisms remain to be elucidated, the data imply that the observed synergism is likely not due to gamma-induced cell cycle arrest or to PDT-induced inhibition of DNA repair. A plausible mechanism is the combined activation of apoptotic and necrotic pathways, however, other mechanisms, especially those involving cellular oxygenation status, cannot be ruled out.

PDT and Hyperthermia

Due to the rapid attenuation of light in biological tissues, high laser powers are required to achieve threshold light fluences at cm depths in the tumor or resection margin. Since most of the optical energy is converted to heat, tissues in close proximity to the light source are likely to undergo significant heating. Hyperthermia is thus an unavoidable effect of high-fluence rate PDT and, therefore, knowledge of potentiation effects between the two modalities may help optimize PDT efficacy.

In contrast to PDT, hypoxic cells have been shown to be very sensitive to hyperthermia [35] and therefore it is highly probable that combination therapies involving these modalities could improve the response of heterogeneous tumors with hypoxic regions.

ALA-PDT and hyperthermia (40–46°C) have been shown to interact synergistically in both rat and human glioma spheroids if the therapies are given concurrently [36]. Neither sub-threshold fluence PDT (<25 J/cm^2) nor temperatures below 49°C inhibited spheroid growth. The degree of synergism increased with both increasing temperature and light fluence. Apoptosis was found to be the primary mode of cell death following combined treatment. The high degree of thermoresistance of both spheroid types was attributed to the close 3-D contact between cells (the so-called contact effect) which has been shown to confer increased resistance of cells to various therapies including hyperthermia [11,37].

Although the mechanism of synergism between PDT and hyperthermia is unknown, it may be due to the concerted action of both treatment modalities on cellular proteins [38]. For example, it has been shown that PDT can induce

photooxidation of intracellular enzymes, such as glyceraldehyde-3-phosphatase dehydrogenase and cytochrome c oxidase [39]. As a result, the enzymes undergo a conformational change which, in turn, affects their susceptibility for thermal inactivation. The net effect of PDT is thus to lower the activation energy of protein denaturing thus making the proteins more susceptible to thermal damage. The observation of high levels of apoptotic cell death following combined hyperthermia and PDT [36] is consistent with this hypothesis since these proteins can be found in the mitochondrial membrane and ALA-induced PpIX has significant mitochondrial localization [40].

AN IN VITRO MODEL OF TUMOR INVASION

Although MCSs have been used primarily to evaluate the effects of PDT on cell growth, they are also well-suited for investigating the utility of therapies on tumor cell invasion which is a hallmark of malignant gliomas, such as GBM. Malignant gliomas are characterized by a large central volume of extensive necrosis surrounded by a dense shell of invasive cells which typically migrate beyond the therapeutic margins resulting in tumor recurrence. Effective treatment modalities should therefore target not only cellular growth but also the migration characteristics of glioma cells.

Several in vitro models have been developed to study glioma cell invasive behavior [41,42]. For example, simple artificial substrates consisting of collagen gels have commonly been employed to examine the effects of ionizing radiation on cell infiltration [43,44]. Such a model has also recently been used to examine the effects of sub-lethal ALA-mediated PDT on glioma cells migrating from organotypic MCS spheroids [45]. In that study, human glioma spheroids of 400–500 μm diameter were placed in a 70% Type I rat tail collagen matrix and cell migration distance from the central spheroid was recorded as a function of light fluence used during ALA-PDT. Migration of cells from an untreated spheroid is shown in Figure 1. Migration distances typically ranged between 300 and 400 μm 24 hours following spheroid implantation. Cultures were terminated 4–5 days following implantation when migration ceased.

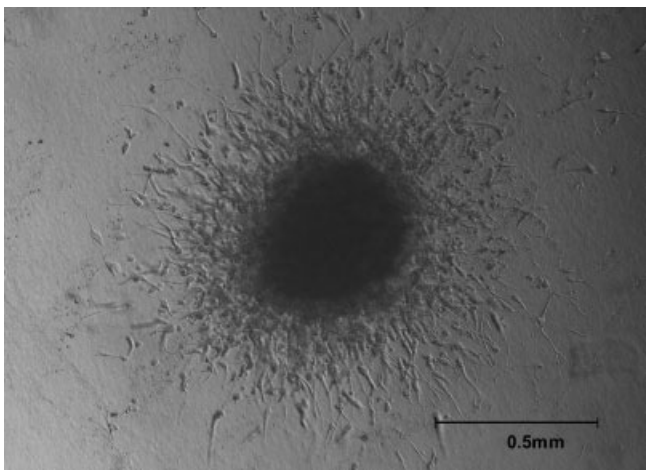

Fig. 1. Photomicrograph of human glioma cell invasion into a rat tail collagen matrix on day 2 of culture. The detached cells migrated into the gel in all three dimensions.

The effect of ALA-PDT on glioma cell invasion is shown in Figure 2. The inhibition of migration observed at high light fluences (12 and 25 J/cm^2) was attributed to the cytotoxic effects of these treatments. Of particular interest is the observation that a light fluence of 6 J/cm^2 resulted in significant inhibition of cell migration, but neither prevented spheroid growth nor was it cytotoxic to the migrating cells.

Since it is difficult to study invasiveness independently of proliferative capacity in an assay of duration longer than the cell doubling time, some control cultures employed spheroids incubated with Mitomycin C prior to implantation. This drug inhibits cellular proliferation, ensuring that the number of cells scored as invasive were entirely due to migration. No significant difference in invasion distance was observed when using either untreated or Mitomycin C-treated spheroids. This observation agrees with the findings of Giese et al. [46] who showed that migrating cells are characterized by decreased proliferation rates compared with the high cell density colony being examined.

Results similar to those reported here have also been obtained by Jiang et al. [47] who used a spheroid confrontation assay to show that sub-cytotoxic Photofrin PDT of co-cultures consisting of human ^{87}U glioma spheroids and fetal rat brain aggregates significantly reduces tumor invasiveness. Taken together, the two studies indicate that sub-lethal PDT can be an effective inhibitor of glioma cell invasion.

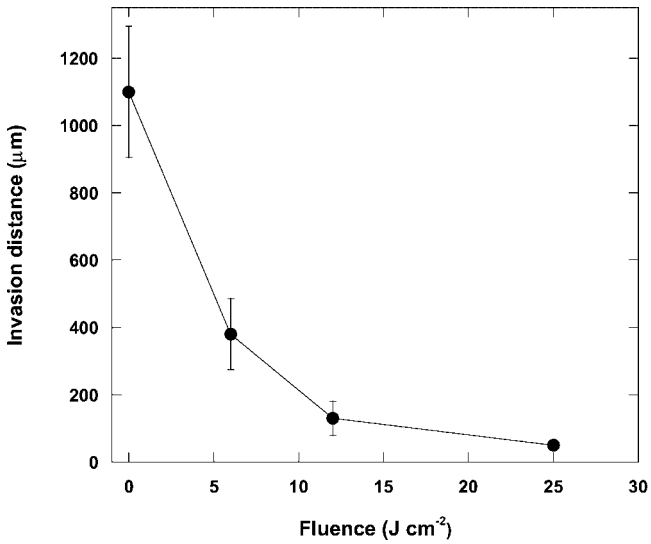

Fig. 2. Invasion distance versus light fluence for human glioma spheroids implanted in a rat collagen matrix. Treatment was initiated 24 hours following spheroid implantation. Individual cultures were incubated in ALA (1,000 μg/ml) for approximately 4 hours and thereafter were irradiated with 635-nm light from a diode laser. Migration distances were scored 4 days after treatment. Values are mean ± SEM. $n = 4$ for each point.

The mechanism by which PDT inhibits glioma cell invasion has not been elaborated. Several mechanisms have been proposed, such as the expression of integrins which bind to permissive substrates initiating the proteolytic and motility necessary for cell migration [48]. Degradation of the surrounding extracellular matrix is necessary for tumor cell migration and matrix-metalloproteinases seem particularly important in this context [49]. Adhesion and motility through permissive substrates in basement membranes might explain the ability of glioma cells to spread along blood vessels and white matter tracts [50]. PDT could conceivably inhibit several of these mechanisms and further studies along these lines are clearly indicated.

A VASCULARIZED MCS MODEL

The chick chorioallantoic membrane (CAM) is an ideal system for the study of PDT-induced vascular damage [51–56], growth and neovascularization of tumor nodules and tumor cell suspensions [57–62], and for the assessment of angiogenic activity [63,64]. Due to its simplicity, this in vivo system represents an attractive alternative to animal studies seeking to optimize PDT dosimetric parameters. The development of an in vivo spheroid/CAM system ideally suited for studies of PDT-induced vascular effects has recently been described [65]. In this model, 1.0-mm diameter human glioma spheroids are placed on a 7-day-old CAM. As illustrated in Figure 3, spheroid neovascularization is clearly evident 7 days after implantation and histological sections (Fig. 4) obtained at that time show that the vasculature penetrates the tumor spheroid. The observed neovascularization is likely not due to non-specific inflammatory reactions that have been observed following spheroid grafting [66]. Such reactions are rare when spheroids are grafted as soon as the CAM begins to develop, while the host's immune system is relatively immature [67].

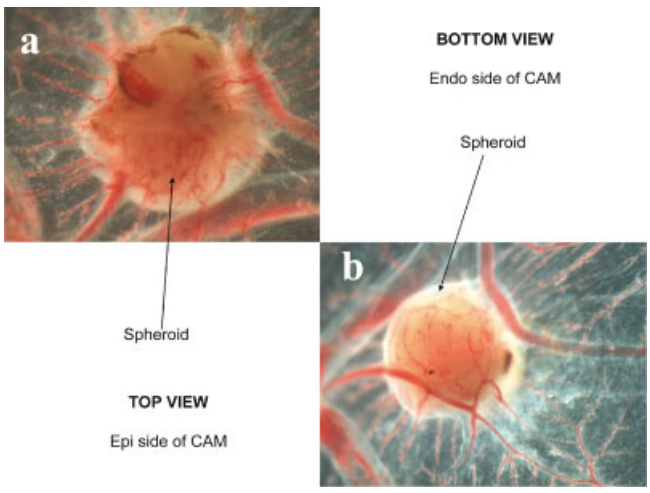

Fig. 3. Photomicrograph showing spheroid vascularization. **a**: Top view—epi side of CAM. **b**: Bottom view—endo side of CAM. Spheroids (indicated by arrows) were implanted on day 7 of chick development. The images were acquired 7 days following spheroid implantation. [Figure can be viewed in color online via www.interscience.wiley.com.]

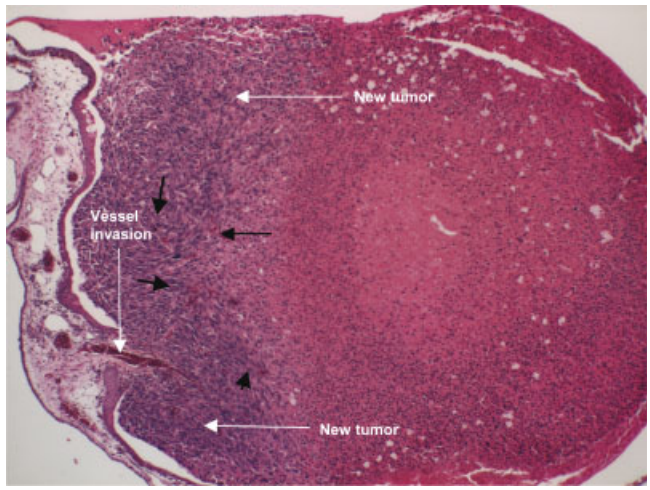

Fig. 4. H&E section of a vascularized spheroid (10× magnification) removed from the CAM 7 days post-implantation. The original spheroid is on the right. Note the acellular necrotic core and the cell-rich new tumor growth on the left side of the image. Vascular components infiltrating the new tumor growth are indicated by black arrows. [Figure can be viewed in color online via www.interscience.wiley.com.]

Although the CAM model is an economical alternative to animal studies, it has a number of drawbacks. Perhaps the most severe of these is the relatively short time window (approximately 10 days) over which studies can be performed. The CAM is formed at an embryo age (EA) of between 4 and 5 days; angiogenesis is typically complete at EA 9. Although the chick can hatch as late as EA 20, observation is commonly terminated at EA 17 when the chick immunological system becomes functional.

AN IN VIVO MCS MODEL

Invasiveness and diffuse infiltrative growth are hallmarks of brain tumors of glial lineage. Human glioma cell lines are relatively easily established from their respective tumors and can be grown in both in vitro culture and as subcutaneous tumors in immunodeficient animals. Glioma cell lines inoculated into the brains of such animals often result in tumor growth, but because of the clonal origin of the cell lines, the resulting tumors may not be fully representative of the original tumors in patients. Many of these cell line-derived tumors have the characteristic appearance of well-defined lesions, such as metastatic brain tumors, and their relevance in glioma research is therefore questionable. Alternatively, fresh brain tumor tissue cultured as organotypic three-dimensional spheroids in vitro may be more appropriate as they have been shown to retain morphologic properties and characteristics of the biopsied tumor. This has been demonstrated in an in vivo model representative of human brain tumors, involving the injection of biopsy-derived tumor spheroids into the brains of immunodeficient nude rats [68]. This study

demonstrated that tumors growing in the brains of nude rats clearly paralleled the histological appearance of the original human tumor biopsies obtained from five different patients. This indicates that the phenotype of the human tumor is preserved in spheroid development as opposed to that seen in monolayers derived from biopsy material. Furthermore, it was shown that the growth patterns and migration characteristics of the human tumors growing in nude rats closely mimicked those of human malignant gliomas. For example, many of the tumors were widely disseminated, invasive in nature, and resulted in the destruction of the normal architecture of the corpus callosum and adjacent structures. In addition, tumor cell migration along the fiber tracts of the corpus callosum and into the contralateral hemisphere was found, but no invasion into the meninges or the calvarium was observed. Even when the tumors were large and caused asymmetry of the hemispheres, none of them crossed the midline by bridging the sagittal fissure directly, but migrated along the corpus callosum to the contralateral hemisphere—migration patterns typical of human GBM.

FUTURE TRENDS: IN SILICO TESTING OF TREATMENT EFFECTS

Several attempts have been made to describe the growth of MCS using computer simulations (in silico). Although it is beyond the scope of this review to go into details of these previously published works, we feel it may be of value to describe briefly our ongoing studies in this direction. The motivation for this type of work is the possibility that new insights will become apparent in a short time frame if an accurate and predictive computer model can be developed. Such a model should be capable of predicting the effects of various treatment modalities, such as chemotherapy, ionizing radiation, and PDT. Since we are specifically interested in repetitive and very low fluence rate PDT, time-consuming modalities to test either in vitro or in vivo, the ability to optimize treatment parameters in silico would be of benefit.

Although the intracellular and extracellular dynamics that govern tumor growth and invasiveness in vivo remain poorly understood, tumor morphogenesis may be a function of marginally stable environmental conditions caused by spatial variations in cell nutrients, oxygen, and growth factors. Our mathematical model based on parameters that directly describe tumor cell cycle and biology has led to the hypothesis that tumor morphology is determined by the competition between heterogeneous cell proliferation (driving shape instability) and invasive tumor morphologies, on the one hand, and stabilizing cell–cell and cell–matrix adhesion forces on the other [69–71].

The model has been applied to predict glioma spheroid morphology and shows that spheroid growth is only marginally stable. Unbounded growth of spheroids and invasion has been observed in vitro under certain conditions and has verified this prediction [72].

Employing this model, a dimensionless parameter $A = \lambda_D/\lambda_M$ that controls overall tumor size has been defined. Here, λ_M is the rate of accumulation of tumor cell mass due to cell mitosis and λ_D is the death rate that describes disintegration of cell mass and radial effusion of intracellular fluid away from the central necrotic region.

Another dimensionless parameter $G = \lambda_M/\lambda_R$ controls morphology stability where λ_R is a relaxation rate associated with cell adhesion. For simplicity, the following assumptions have been made: (1) viable cell mass density is uniform in the tumor, and (2) regions become necrotic where nutrient and oxygen concentrations fall below some specified minimum threshold.

By fitting the model to in vitro data of spheroid growth curves and histology, it is possible to calculate a diffusion length of nutrient, oxygen, and growth factors ($L \approx 100\,\mu m$), an average proliferation rate ($\lambda_M \approx 1$ per day), a range of values for the death parameter ($0.26 \leq A \leq 0.38$), and a range of values where morphologically stable spheroids can exist ($0.6 \leq G \leq 0.9$). Spheroids with values of G above this range will not be stable as cell adhesion forces are too weak. In the computer simulations, compact spheroid morphology was achieved for values of G within the stable region. For an unstable case ($G > 0.9$), snapshots of the evolution of a tumor spheroid are shown in Figure 5. The outer boundary tracks the surface of the spheroid; the inner boundary encloses regions of hypoxia, where necrotic cells can be found. A thin rim (thickness roughly equal to L) of viable and actively proliferating cells is predicted, surrounding a large hypoxic core as was observed in vitro. The irregularities arising on the spheroid surface arise from random oscillations of the positions of the cells. These oscillations introduce low-wave-number perturbations on the spheroid surface, as can be seen in the snapshots from the simulation and in the photographs from the in vitro experiments. In this sense, wave-number refers to the frequency of the cell clusters emanating from the central spheroid. The perturbations grow (large G) leading to formation of subspheroidal structures that eventually separate from the mother spheroid (for comparison, see the photographs from the in vitro experiments). Clusters of spheroids are thus formed that allow the tumor mass to grow to a much larger size and over a much larger region than would have been possible had the spheroid maintained a compact shape and instability had not occurred. If the spheroid remains compact, nutrient and oxygen diffusion limitations to mass growth cause the spheroid to reach a final, stable size. In the last snapshot from the simulation, it is shown that the instability repeats itself on the sub-spheroids, as was also observed in the in vitro spheroid cultures.

It is felt that this type of model that incorporates basic tumor growth kinetics information is capable of representing and predicting tumor response to various forms of therapy including PDT. In preliminary studies, in vitro tumor growth and drug response of Doxorubicin-sensitive and resistant MCF-7 breast cancer cells have been measured (data not shown). The results of parameter-based statistics were used to define input variables to our in silico model, and computer simulations to measure the drug response predicted by the model have been run. The computer model could accurately predict the in vitro

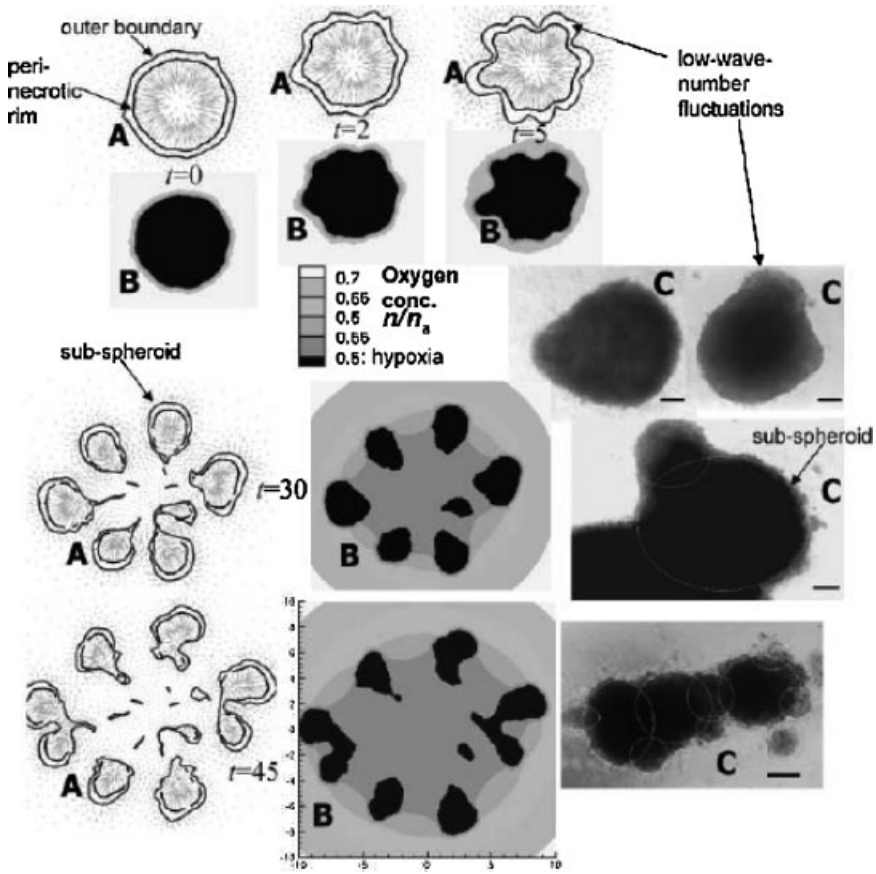

Fig. 5. Spheroid morphologies from computer simulations and experiments. Low-wave-number instabilities arise on spheroid surfaces eventually leading to the development and separation of sub-spheroids. Simulation snapshots (length rescaled with diffusion length L, time t rescaled with mitosis time $1/\lambda_M^{-1} \approx$ 1 day) showing the outer boundary and inner peri-necrotic rims (**A**), and local levels of diffusing substances (**B**), such as oxygen or glucose. Photographs (**C**): glioma spheroids growing in culture. Sub-spheroids are highlighted in middle and bottom photographs. Bar = 130 μm.

response of drug-sensitive and -resistant MCF-7 breast cancer cells. The model also predicted that oxygen and nutrient gradients in the tumor micro-environment, whether naturally occurring or induced by treatment, could increase the invasive capability of tumor cells and destabilize tumor morphology as previously described. Current treatment modalities, (in particular anti-angiogenic therapy), may trigger local hypoxia causing invasive instability. This effect could also contribute to acquired therapy resistance by increasing the population of quiescent cells. It appears then that a rigorously, experimentally calibrated computer model, can be accurately predictive of in vitro tumor response to therapeutic modalities like chemotherapy. We feel that the validation of this model for chemotherapy will allow its extension to other treatment modalities, in particular PDT. This type of validation begins the path to computational modeling and more efficient prediction of in vivo tumor response to therapy.

SUMMARY

MCSs represent an in vitro system of intermediate complexity between monolayer cultures and tumors in situ. MCSs are characterized by oxygen, nutrient, and pH gradients that mimic those found in vivo and therefore, it is hardly surprising that they are structurally similar to solid tumors. In contrast to more complex animal models, MCSs allow for direct monitoring of the anti-tumor cell effects of treatments, separate from the influence of the tumor vasculature, immunological reactions, and other in vivo effects.

There are a number of limitations that must be considered when using MCS in PDT investigations. Perhaps the most important of these is the dependence of cellular growth kinetics and oxygenation properties on the type of spheroid culture technique used. It is also important to realize that the extracellular matrix in MCS originates from tumor cells whereas in vivo, it is produced primarily by host cells. This implies a differential expression of genes producing extracellular matrix constituents.

MCSs have played a key role in our understanding of how basic parameters, such as oxygen levels, photosensitizer concentrations, light fluence, and fluence rate contribute to the overall PDT effect. MCSs have proven especially useful in furthering our understanding of photobleaching

kinetics—an important parameter for non-invasive PDT dosimetry. Spheroids have also been shown to be useful in a number of PDT studies investigating the utility of repetitive treatments and combined therapies. The observation that PDT may be an effective inhibitor of tumor cell invasion suggests that this type of therapy may be particularly useful in the management of patients with malignant gliomas. The development of vascularized spheroid models provides new opportunities for investigating the effects of PDT on tumor vasculature and combination therapies involving PDT and anti-angiogenic treatments. The observation that MCS cultured from patient biopsies have been shown to retain the morphologic properties and characteristics of the original tumor, has lead to the development of improved brain tumor models that can be used to more accurately gage the efficacy of investigational therapies, such as PDT. Finally, in silico models incorporating basic tumor growth kinetics information may be capable of predicting tumor response to a number of therapies including PDT. Such models have predicted a number of counterintuitive responses to treatment including therapy-induced resistance and tumor cell invasion. If true, these predictions suggest that many current treatment regimens (and investigational therapies) may not be optimal and, as such, in silico models certainly warrant further study.

ACKNOWLEDGMENTS

Steen Madsen is grateful for the support of the UNLV Office of Research and the UNLV Cancer Research Center. Henry Hirschberg is grateful for the support of the Norwegian Cancer Society and the Norwegian Research Council (NFR).

REFERENCES

1. Inch WR, McCredie JA, Sutherland RM. Growth of nodular carcinoma in rodents compared with multi-cell spheroids in tissue culture. Growth 1970;34:271–282.
2. Sutherland RM, McCredie JA, Inch WR. Growth of multicellular spheroids in tissue culture as a model of nodular carcinomas. J Natl Cancer Inst 1971;46:113–120.
3. Sutherland RM. Cell and environment interactions in tumor microregions: The multicell spheroid model. Science 1988; 240:177–184.
4. Santini MT, Rainaldi G, Indovina PL. Multicellular tumor spheroids in radiation biology. Int J Radiat Biol 1999;75:787–799.
5. Kunz-Schughart LA, Kreutz M, Knuechel R. Multicellular spheroids: A three-dimensional *in vitro* culture system to study tumour biology. Rev Int J Exp Pathol 1998;79:1–23.
6. Casciari JJ, Rasey JS. Determination of the radiobiologically hypoxic fraction in multicellular spheroids from data on the uptake of [3H]fluoromisonidazole. Radiat Res 1995;141:28–36.
7. Franko AJ, Parliament MB, Allalunis-Tumer MJ, Wolokoff BG. Variable presence of hypoxia in M006 human glioma spheroids and in spheroids and xenografts of clonally derived sublines. Br J Cancer 1998;78:1261–1268.
8. Gorlach A, Acker H. pO_2- and pH-gradients in multicellular spheroids and their relationship to cellular metabolism and radiation sensitivity of malignant human tumor cells. Rev Biochem Biophys Acta 1994;29:105–112.
9. Gross MW, Karbach U, Groebe K, Franko AJ, Mueller-Kieser W. Calibration of misonidazole labeling by simultaneous measurement of oxygen tension and labeling density in multicellular spheroids. Int J Cancer 1995;61:567–573.
10. Mueller-Klieser W. Three-dimensional cell cultures: From molecular mechanisms to clinical applications. Am J Physiol 1997;273:C1109–C1123.
11. Olive PL, Durand RE. Drug and radiation resistance in spheroids: Cell contact and kinetics. Cancer Metastasis Rev 1994;13:121–138.
12. Santini MT, Rainaldi G, Indovina PL. Apoptosis, cell adhesion and the extracellular matrix in the three-dimensional growth of multicellular tumor spheroids. Crit Rev Onc/Hem 2000;36:75–87.
13. Wilson BC, Patterson MS, Lilge L. Implicit and explicit dosimetry in photodynamic therapy: A new paradigm. Lasers Med Sci 1997;12:182–199.
14. Christensen T, Moan J, Sandquist T, Smedshammer L. Multicellular spheroids as an in vitro model system for photoradiation therapy in the presence of Hpd. Prog Clin Biol Res 1984;170:381–390.
15. Jeeves WP, Wilson BC, Smith P, Ens K, Spiegl P. Growth delay studies of the response of V-79 multicell spheroids exposed to DHE and red light. Photochem Photobiol 1987; 46(5):723–728.
16. West CM. Size-dependent resistance of human tumour spheroids to photodynamic treatment. Br J Cancer 1989; 59(4):510–514.
17. West CM, Moore JV. Flow cytometric analysis of intracellular hematoporphyrin derivative in human tumour cells and multicellular spheroids. Photochem Photobiol 1989;50(5): 665–669.
18. Purkiss SF, Grahn MF, Turkish M, Macey MG, Williams NS. In vitro modulation of hematoporphyrin derivative photodynamic therapy on colorectal carcinoma multicellular spheroids by verapamil. Br J Surg 1992;79(2):120–125.
19. West CM, Moore JV. Mechanisms behind the resistance of spheroids to photodynamic treatment: A flow cytometric study. Photochem Photobiol 1992;55(3):425–430.
20. Coutier S, Mitra S, Bezdetnaya LN, Parache RM, Georgakoudi I, Foster TH, Guillemin F. Effects of fluence rate on cell survival and photobleaching in meta-tetra-(hydroxyphenyl)-chlorin-photosensitized Colo 26 multicell tumor spheroids. Photochem Photobiol 2001;73(3):297–303.
21. Huygens A, Huyghe D, Bormans G, Verbruggen A, Kamuhabwa AR, Roskams T, deWitte PA. Accumulation and photocytotoxicity of hypericin and analogs in two- and three-dimensional cultures of transitional cell carcinoma cells. Photochem Photobiol 2003;78(6):607–614.
22. Bigelow CE, Mitra S, Knuechel R, Foster TH. ALA- and ALA-hexylester-induced protoporphyrin IX fluorescence and distribution in multicell tumor spheroids. Br J Cancer 2001;85: 727–734.
23. Kloek J, Beijersbergen van Henegouwen GMJ. Prodrugs of 5-aminolevulinic acid for photodynamic therapy. Photochem Photobiol 1996;64:994–1000.
24. Hirschberg H, Sun C-H, Tromberg BJ, Madsen SJ. ALA- and ALA-ester-mediated photodynamic therapy of human glioma spheroids. J Neurooncol 2002;57:1–7.
25. Foster TH, Hartley DF, Nichols MG, Hilf R. Fluence rate effects in photodynamic therapy of multicell tumor spheroids. Cancer Res 1993;53:1249–1254.
26. Madsen SJ, Sun C-H, Tromberg BJ, Wallace VP, Hirschberg H. Photodynamic therapy of human glioma spheroids using 5-aminolevulinic acid. Photochem Photobiol 2000;72:128–134.
27. Marchal S, Fadloun A, Maugain E, D'Hallewin MA, Guillemin F, Bezdetnaya L. Necrotic and apoptotic features of cell death in response to Foscan photosensitization of HT29 monolayer and multicell spheroids. Biochem Pharmacol 2005;69(8):1167–1176.
28. Georgakoudi I, Nichols MG, Foster TH. The mechanism of Photofrin photobleaching and its consequences for photodynamic dosimetry. Photochem Photobiol 1997;65:135–144.

29. Georgakoudi I, Foster TH. Singlet oxygen- versus nonsinglet oxygen-mediated mechanisms of sensitizer photobleaching and their effects on photodynamic dosimetry. Photochem Photobiol 1998;67:612–625.
30. Georgakoudi I, Foster TH. Effects of the subcellular redistribution of two nile blue derivatives on photodynamic oxygen consumption. Photochem Photobiol 1998;68:115–122.
31. Finlay JC, Mitra S, Patterson MS, Foster TH. Photobleaching kinetics of Photofrin in vivo and in multicell tumour spheroids indicate two simultaneous bleaching mechanisms. Phys Med Biol 2004;49:4837–4860.
32. Madsen SJ, Sun C-H, Tromberg BJ, Hirschberg H. Repetitive 5-aminolevulinic acid-mediated photodynamic therapy on human glioma spheroids. J Neurooncol 2003;62:243–250.
33. Madsen SJ, Sun C-H, Tromberg BJ, Hirschberg H. Development of a novel indwelling balloon applicator for optimizing light delivery in photodynamic therapy. Lasers Surg Med 2001;29:406–412.
34. Madsen SJ, Sun C-H, Tromberg BJ, Yeh AT, Sanchez R, Hirschberg H. Effects of combined photodynamic therapy and ionizing radiation on human glioma spheroids. Photochem Photobiol 2002;76:411–416.
35. Song CW. Effect of local hyperthermia on blood flow and microenvironment. Cancer Res 1984;44:4721s–4730s.
36. Hirschberg H, Sun C-H, Tromberg BJ, Yeh AT, Madsen SJ. Enhanced cytotoxic effects of 5-aminolevulinic acid-mediated photodynamic therapy by concurrent hyperthermia in glioma spheroids. J Neurooncol 2004;70:289–299.
37. Wigle JC, Sutherland PM. Increased thermoresistance developed during growth of small multicellular spheroids. J Cell Physiol 1985;122:281–289.
38. Prinsze C, Penning LC, Dubbelman TMAR, VanSteveninck J. Interaction of photodynamic treatment and either hyperthermia and ionizing radiation and of ionizing radiation and hyperthermia with respect to cell killing of L929 fibroblasts, Chinese hamster ovary cells and T24 human bladder carcinoma cells. Cancer Res 1992;52:117–120.
39. Prinsze C, Dubbelman TMAR, VanSteveninck J. Potentiation of the thermal inactivation of glyceraldehydes-3-phosphate dehydrogenase by photodynamic treatment. A possible model for the synergistic interaction between photodynamic therapy and hyperthermia. Biochem J 1991; 276:357–362.
40. Verma A, Facchina SL, Hirsch DJ, Song S-Y, Dillahey LF, Williams JR, Snyder SH. Photodynamic tumor therapy: Mitochondrial benzodiazepine receptors as a therapeutic target. Mol Med 1998;4:40–48.
41. Easty GC, Easty GM. In vivo and in vitro models of invasion. In: Mareel MM, Calman KC, editors. Invasion. Experimental and Clinical Implications. New York: Oxford University Press, 1984: pp 24–62.
42. Evans CW. In vitro model systems for the study of tumor cell invasion and metastasis. The Metastatic Cell: Behavior and Biochemistry. New York: Chapman and Hall, 1991: pp 293–331.
43. Bauman GS, Fisher BJ, MacDonald W, Amberger VR, Moore E, DelMaestro RM. Effects of radiation on a three dimensional model of malignant glioma invasion. Int J Dev Neurosci 1999;17(5–6):643–651.
44. Bauman GS, MacDonald W, Moore E, Ramsey DA, Fisher BJ, Amberger VR, Del Maestro RM. Effects of radiation on a model of malignant glioma invasion. J Neurooncol 1999;44: 223–231.
45. Hirschberg H, Sun C-H, Madsen SJ. Reduction of invasiveness of human glioma cells by ALA mediated photodynamic therapy. Proc SPIE 2006;6078:481–486.
46. Giese A, Bjerkvig R, Berens ME, Westphal M. Cost of migration: Invasion of malignant gliomas and implications for treatment. J Clin Oncol 2003;21(8):1624–1636.
47. Jiang F, Chopp M, Katakowski M, Cho K-K, Yang X, Hochbaum N, Tong L, Mikkelsen T. Photodynamic therapy with Photofrin reduces invasiveness of malignant human glioma cells. Lasers Med Sci 2002;17:280–288.
48. Rao JS. Molecular mechanisms of glioma invasiveness: The role of proteases. Nat Rev Cancer 2003;3(7):489–501.
49. Uhm JH, Dooley NP, Villemure JG, Yong VW. Mechanisms of glioma invasion: Role of matrix-metalloproteinases. Can J Neuro Sci 1997;24:3–15.
50. Bjerkvig R, Pederson PH, Terzis AJ. Tissue specific invasion of brain tumors. J Neurooncol 1992;12:258 (abstract).
51. Gottfried V, Lindenbaum ES, Kimel S. Vascular damage during PDT as monitored in the chick chorioallantoic membrane. Int J Radiat Biol 1991;60:349–354.
52. Toledano H, Edrei R, Kimel S. Photodynamic damage by liposome-bound porphycenes: Comparison between in vitro and in vivo models. J Photochem Photobiol B: Biol 1998;42: 20–27.
53. Srauss WSL, Sailer R, Schneckenburger H, Akguen N, Gottfried V, Chetwer L, Kimel S. Photodynamic efficacy of naturally occurring porphyrins in endothelial cells in vitro and microvasculature in vivo. J Photochem Photobiol B: Biol 1997;39:176–184.
54. Gottfried V, Davidi R, Averbuj C, Kimel S. In vivo damage to chorioallantoic membrane blood vessels by porphycene-induced photodynamic therapy. J Photochem Photobiol B: Biol 1995;30:115–121.
55. Hammer-Wilson MJ, Akian L, Espinoza J, Kimel S, Berns MW. Photodynamic parameters in the chick chorioallantoic membrane (CAM) bioassay for topically applied photosensitizers. J Photochem Photobiol B: Biol 1999;53: 44–52.
56. Hammer-Wilson MJ, Cao D, Kimel S, Berns MW. Photodynamic parameters in the chick chorioallantoic membrane (CAM) bioassay for photosensitizers administered intraperitoneally (IP) into the chick embryo. Photochem Photobiol Sci 2002;1:721–728.
57. Knighton D, Ausprunk D, Tapper D, Folkman J. Avascular and vascular phases of tumor growth in the chick embryo. Br J Cancer 1977;35:347–356.
58. Ishiwata I, Ishiwata C, Soma M, Ono I, Nakaguchi T, Ishikawa H. Tumor angiogenic activity of gynecologic tumor cell lines on the chorioallantoic membrane. Gynecol Oncol 1988;29:87–93.
59. Preminger GM, Koch WF, Fried FA, Mandell J. Chorioallantoic membrane grafting of the embryonic murine kidney. An improved in vitro technique for studying kidney morphogenesis. Invest Urol 1981;18:377–381.
60. Petruzzelli GJ, Snyderman CH, Johnson JT, Myers EN. Angiogenesis induced by head and neck squamous cell carcinoma xenografts in the chick embryo chorioallantoic membrane model. Ann Otol Rhinol Laryngol 1993;102:215–221.
61. Kirchner LM, Schmidt SP, Gruber BS. Quantitation of angiogenesis in the chick chorioallantoic membrane model using fractal analysis. Microvascular Res 1996;51:2–14.
62. Hornung R, Hammer-Wilson MJ, Kimel S, Liaw L-H, Tadir Y, Berns MW. Systemic applications of photosensitizers in the chick chorioallantoic membrane (CAM) model: Photodynamic response of CAM vessels and 5-aminolevulinic acid uptake kinetics by transplantable tumors. J Photochem Photobiol B: Biol 1999;49:41–49.
63. Barnhill RL, Ryan J. Biochemical modulation of angiogenesis in the chorioallantoic membrane of the chick embryo. J Invest Derm 1983;81:485–488.
64. Vu T, Smith CF, Burger PC, Klintworth GK. An evaluation of methods to quantitate the chick chorioallantoic membrane assay in angiogenesis. Lab Invest 1974;53:499–508.
65. De Magalhães N, Liaw L-HL, Li L, Liogys A, Madsen SJ, Hirschberg H, Tromberg BJ. Investigating the effects of combined photodynamic and anti-angiogenic therapies using a three-dimensional *in vivo* brain tumor system. Proc SPIE 2006;6078:503–508.
66. Ribatti D, Nico B, Vacca A, Roncali L, Burri PH, Djonov V. Chorioallantoic membrane capillary bed: A useful target for studying angiogenesis and anti-angiogenesis. Anat Rec 2001; 264:317–324.
67. Leene W, Duyzings MJM, Von Steeg C. Lymphoid stem cell identification in the developing thymus and bursa of Fabricius of the chick. Z Zellforcsh 1973;136:521–533.

68. Engebraaten O, Hjortland GO, Hirschberg H, Fodstad O. Growth of precultured human glioma specimens in nude rat brain. J Neurosurg 1999;90:125–132.
69. Cristini V, Frieboes HB, Gatenby R, Caserta S, Ferrari M, Sinek J. Morphological instability and cancer invasion. Clin Cancer Res 2005;11(19):6772–6779.
70. Cristini V, Lowengrub J, Nie Q. Nonlinear simulation of tumor growth. J Math Biol 2003;46:191–224.
71. Zheng X, Wise S, Cristini V. Nonlinear simulation of tumor necrosis, neo-vascularization and tissue invasion *via* an adaptive finite-element/level-set method. Bull Math Biol 2005;67:211–259.
72. Frieboes H, Zheng X, Sun C-H, Tromberg B, Gatenby R, Cristini V. An integrated computational/experimental model of tumor invasion. Cancer Res 2006;66(3):1–8.